The relationship between landslide distribution and the superposition of geology, geomorphology, and hypocenter: The mid Niigata earthquake in 2004

by

Hiroshi P. Sato[1 †], Tatsuo Sekiguchi[1], Ryoichi Kojiroi[1],
Yoshinori Suzuki[2], Makoto Iida[2] and Masanori Sugiyama[3]

ABSTRACT

The mid Niigata prefecture earthquake in 2004, which was caused by the slip off of the reverse fault, brought many landslides in and around Yamakoshi village. Aerial photographs taken after the earthquake were interpreted to inventory the landslides, in the end a total of 1,353 landslides were identified. The estimated fault plane of the main shock and the associated slip off length were overlaid on the landslide inventory map. As a result, it appears that the landslides are concentrated more in the hanging wall than in the foot wall. However, there is no clear relation between slip off length and landslides density.

Furthermore, geological map was overlaid on the inventory map. The two zones where landslides are concentrated were identified. The northwestern zone occurs on the northwestern wing of the anticline. The southeastern zone lies along the synclinal axis. Landslide density was calculated according to geological formations, but it was not easy to find the specific geological formation where many landslides were concentrated.

The topographic volume change between before and after the earthquake was calculated in the landslides in Higashi-Takezawa, Yamakoshi village. It was found that the apparent transported volume from the source area to the accumulated area was ca. 550 thousand m^3.

KEYWORDS: Aerial photograph, Interpretation, Landslide, Mid Niigata prefecture earthquake

1. INTRODUCTION

The mid Niigata prefecture earthquake occurred in northwestern Japan at 17:56 JST on October 23, 2004. The epicenter of the main shock (magnitude 6.8) is located at 37°17.4’N; 138°52.2’E at a depth of 13 km [1], many severe aftershocks occurred. The earthquake was caused by the slip off of the reverse fault, and the fault planes were estimated ([2], [3]).

2. STUDY AREA

The study area is the rectangular shown in Fig. 1. Yamakoshi village, where many landslides occurred, is located on the Higashiyama Hill at heights of 300-700 m. The known active faults stretch from north-northeast to south-southwest in the study area ([4], [5], [6]).

The geology in the study area consists of a thick sequence of Miocene to lower Pleistocene sediments with well-developed terraces [7]. Alluvial plane deposits exist along the rivers. Active folds are common, and the sequence of hills and basins were formed by an active fold [8].

3. METHOD

3.1 Aerial Photographs Interpretation

To prepare landslide inventory map, 1/10,000-1/13,000 scale aerial photographs taken in 24 and 28 October 2004 were used. Interpreted landslides were mapped onto the 1:25,000 topographical map, which is issued by Geographical Survey Institute. As a result, landslides with a minimum map scale size of 1mm by 1mm were detected.

[1] Geography and Crustal Dynamics Research Center, Geographical Survey Institute, Tsukuba-shi, Ibaraki-ken 305-0811 Japan

[†] Senior Researcher

[2] Geographic Department, ditto

[3] Planning Department, ditto

In mapping the identified landslides, we tried to identify as much as possible small scale landslides were. However, in those cases where two or more small scale landslides occur adjacently, they were mapped as a single landslide.

3.2 Overlaying Other Data on the Landslide Inventory Map

3.2.1 Earthquake Source Data

To investigate the relationship between landslides distribution and earthquake source, the epicenters and magnitude of the main shock and aftershocks were overlaid on the landslide inventory map. Furthermore, the estimated fault plane of the main shock and the associated slip off length [3] were overlaid on the inventory map. They gathered seismic waveforms observed by the strong motion seismographs situated around the epicenter, performed inversion on the waveforms, and obtained their results.

3.2.2 Geological Data

To investigate the relationship between landslides distribution and geology, the 1:50,000 scale geological map [7] was selected and digitized. We chose this map as it is the most detailed source of geology available for the area. The digitized area comprises the eastern part of Shinano River and northern part of Uono River, respectively. Landslides triggered by the earthquake are concentrated in the digitized area.

3.2.3 Topographical Data

To calculate the elevation change of the landslide occurred at Higashi-Takezawa, Yamakoshi village ("B" in the Fig. 2), landslide inventory map was overlaid on the 10-meter-grid digital elevation model (DEM) The reason why the Higashi-Takezawa landslide was selected is that its size is large (ca. 8.0 ha in area) and the relative height is high (ca. 150m between the main scarp and the toe of the landslide lobe).

The pre-earthquake DEM (Hokkaido Chizu Co., Ltd) for the landslide was generated (Fig. 3, upper) from a 1:25,000 topographic contour map. The contour map was surveyed by photogrammetry, whose measurement accuracy is 5 m in elevation. The post-earthquake DEM (Aero Asahi Corporation) for the area was generated (Fig. 3, middle) from airborne light detection and ranging (LIDAR) data, whose measurement accuracy is ca. 0.15 m. The airborne LIDAR data were measured on 28 Oct, 2004.

4. RESULTS AND DISCUSSION

4.1 Landslide Inventory Map

The result is shown in Fig. 2. Those areas delineated by lines reflect landslides. Each landslide, including the source, transportation and accumulation areas, was digitized as a single polygon. In the end a total of 1,353 landslides were identified. As shown in Fig. 2, it was found that there are two zones where landslides are concentrated.

Landslides were classified into two categories: landslides with long-traveling flow phenomenon [9] and landslides without the phenomenon. The final tally of landslide with and without the phenomenon was 45 and 1,308, respectively.

4.2 Overlay of Earthquake Source Data

The result of the multi-data overlay is shown in Fig. 4. The epicenter of the main shock is located in the southern part of landslide concentrated zone. In Fig. 4, the estimated fault plane and slip off length on it are projected to the ground, and the slip off length shown in the Fig. 4 was simplified from the original figure. The maximum slip off length was 1.6 m [3].

Although not mentioned by Koketsu et al [3], the northwestern and southeastern edges of the estimated fault plane are 12.9 km and 0.2 km in depth, respectively (Dr. Hikima, personal communication). And the fault plane slipped off from the northwest to southeast. In Fig. 4, it appears that the landslides are concentrated more in the hanging wall than in the foot wall. But to draw a proper conclusion, the landslide distribution should also be investigated in the east side of the study area.

It is expected that the longer the slip off length is, the more violently the ground is jolted, and the more landslides will occur. However, Fig. 4 does not indicate the clear relation between the slip off length and landslides density. To investigate the relationship between landslide distribution and slip off length in detail, it is also necessary to consider the seismic wave propagation.

4.3 Overlay of Geological Data

The result of the overlay is shown in the upper Fig. 5. In the Table 1, the geology, including age and facies are listed. A cross section of the geology is shown in the lower Fig.5. In the upper and lower Fig. 5, the locations “a”, “b” ,and “c” are coincident. In Fig. 5, anticlinal and synclinal axes stretch from north-northeast to south-southwest. These axes are also indicated in the cross section.

Comparing Fig. 5 with Fig. 2, the northwestern landslide-concentrated zone occurs on the northwestern wing of the anticline. The southeastern zone lies along the synclinal axis.

Fig. 6 shows landslide density in each geological formation. Here, the landslides are paid attention to where they overlapped with the geological data. The landslides were classified into the two categories previously explained. The 30 and 797 landslides comprising the 827 represent those with and without long-traveling flow phenomenon.

In the Fig. 6, in the case of landslide with the flow phenomenon, the highest density was 1.64 counts/km^2 in Ks of sandstone, and the density less than 1 counts/km^2 were calculated in the other geological formations. In the case of landslide without flow, the highest density was 12.69 counts/km^2 in Ku2 of sandy mudstone, and the density more than 6 counts/km^2 were calculated in the almost all of the geological formation. However, it is not easy to conclude the localization of the landslide-occurrence by only Fig. 6.

4.4 Overlay of Topographical Data

The lower Fig. 3 were calculated by subtracting the pre-earthquake DEM (Fig. 3, upper) from the post-earthquake DEM (Fig.3, middle). DEM measurement accuracy has been considered, hence a difference between -5 ~ 5 m is defined as no-change. The area “A” in the lower Fig. 3 is the accumulation area, where elevation increased, and when considering upper and middle Fig. 3, the terrain rises into a small hill and a landslide dam in Imo River. The area “S” in the lower Fig. 3 is the source area, where elevation decreased. The slip surface photograph shown in the Fig. 3 was taken in the area of “S”.
The “A” and “S” in the lower Fig. 3 are 29,800 m^2 and 28,300 m^2 in area, respectively. And both “A” and “S” have nearly equal area. The average elevation increase in “A” was 20.26 m in elevation, and the average elevation decrease in “S” was 18.53 m in elevation. The calculated volume increase was 29,800×20.26 = 603,748 m^3 and the loss volume was determined to be 28,300×18.53 = 524,399 m^3. The volume change was 603,748–524,399 = 79,349 m^3.

However this volume should be treated as no-change, because when this volume was divided by the area 29,800 m^2 in “A”, the average change elevation is ca. 2.7 m. This value is within the DEM measurement error. As a result, it was found that the loss volume in the source area balanced with the obtained volume in the accumulated area, and apparent transported volume from “S” to “A” in the lower Fig. 3 was ca.550,000 m^3.

5. CONCLUSIONS

1) The number of the total number of landslides was 1,353 in the whole study area, which was interpreted on the basis of aerial photographs taken after the main shock.
2) It was found that there are the two zonal arrangements where many landslides occurred.
3) It appears that the landslides are concentrated more in the hanging wall than in the foot wall. There was not a clear relationship between the slip off length on the estimated fault plane and landslides density.
4) The landslide density was calculated for each geological formation, but it is not easy to conclude the localization of the landslide-occurrence according to the geological

formation.

5) The volume change between before and after the earthquake was calculated in the landslides in Higashi-Takezawa, Yamakoshi village. It was found that the apparent transported volume was ca. 550 thousand m^3.

6. REFERENCES

1. Japan Meteorological Agency: Press release materials (28th report on November 10), 2004. http://www.seisvol.kishou.go.jp/eq/gaikyo/kaisetsu200411100600.pdf (in Japanese)
2. Geographical Survey Institute: Press release materials on 29 October, 2004. http://www.gsi.go.jp/WNEW/PRESS-RELEASE/2004/1029-3.htm (in Japanese).
3. Koketsu K., Hikima K., Miyake H., Tanaka Y.: The mid Niigata prefecture earthquake in 2004 –strong motion and source process–, 2004. http://taro.eri.u-tokyo.ac.jp/saigai/chuetsu/chuetsu.html (in Japanese)
4. Suzuki Y, Togo M, Watanabe M, Kim HY, Sato H.: Active fault map in urban area at 1:25,000 (Tokamachi), Geographical Survey Institute, 2001. (in Japanese)
5. Tsutumi H, Togo M, Watanabe M, Kim HY, Sato H.: Active fault map in urban area at 1:25,000 (Nagaoka), Geographical Survey Institute, 2001. (in Japanese)
6. Watanabe M, Tsutsumi H, Suzuki Y, Kim HY, Sato H.: Active fault map in urban area at 1:25,000 (Ojiya), Geographical Survey Institute, 2001. (in Japanese)
7. Yanagisawa Y., Kobayashi I., Takeuchi K., Tateishi M., Chihara K., Kato H.: Geology of the Ojiya district, with geological sheet map at 1:50:000, Geological Survey of Japan, 1986. (in Japanese with English abstract)
8. Ota, Y.: Crustal movements in the late Quaternary considered from the deformed terrace plains in northern Japan, Japanese Journal of Geology and Geography, Vol.40, 121-129, 1969.
9. Fukuoka H., Wang G., Sassa K., Wang F. and Matsumoto T.: Earthquake-induced long-traveling flow phenomenon: May 2003 Tsukidate landslide in Japan, Landslides, Vol.1, 151-155, 2004.
10. Geographical Survey Institute: Disaster map at 1:30,000, 2004. (in Japanese)

Table 1 Geology shown in the Fig. 5 (Geology is after [7]).

Geology	Age	Facies and characteristics
Terrace, talus and alluvial cone deposits T	Holocene and Pleistocene	Sand, gravel and silt.
Uonuma Formation U3	Pleistocene	Marine silt, sand and gravel. The U3 is made up of lagoon or bay sediments and barrier sands.
Uonuma Formation U2	Pleistocene	Silt, sand and gravel. The U2 is fluvial deposits composed of silt and channelized thick sand.
Uonuma Formation U1	Pliocene	Thick sequence of gravel, silt and sand. The U1 is presumed to be alluvial fan deposits. The Formation overlies conformably the Wanazu Formation.
Wanazu Formation W	Pliocene	Sandstone. The Formation overlies conformably the Shiroiwa Formation. It consists of poorly stratified fine- to very fine grained sandstone containing mica and pumice fragments.
Shiroiwa Formation S	Pliocene	Sandy mudstone, and thinly interbedded sandy mudstone and fine-grained sandstone (with andesitic volcanic breccia). The Formation conformably rests on the Ushigakubi Formation. The main part of this formation is made up of massive bioturbated sandy mudstone.
Ushigakubi Formation Us	Pliocene	Massive mudstone. The Formation overlies conformably the Kawaguchi Formation. It is predominated by poorly stratified mudstone in the western sing of the anticline. The formation was deposited in lower part of continental slope.
Kawaguchi Foramtion Ks	Pliocene	Sandstone. The Formation is represented by submarine fan deposits.
Kawaguchi Foramtion Ku2	Pliocene	Sandy mudstone interbedded with sandstone. (ditto)
Kawaguchi Foramtion Ku1	Pliocene	Mudstone interbedded with sandstone. (ditto)
Kawaguchi Foramtion Kv	Pliocene	Dacitic volcanic breccia. (ditto)
Kawaguchi Foramtion Kl	Pliocene	Sandstone interbedded with mudstone. (ditto). The Formation overlies conformably the underlying Araya Formation.
Araya Formation A	Pliocene	Dark gray massive mudstone.
Toyagamine Formation Tv	Miocene	Dacite lava, andesitic volcanic breccia and andesite breccia
Nishimyo Formation N	Miocene	Dacitic pyroclastic rocks,mudstone, dacite lava and rhyolite lava

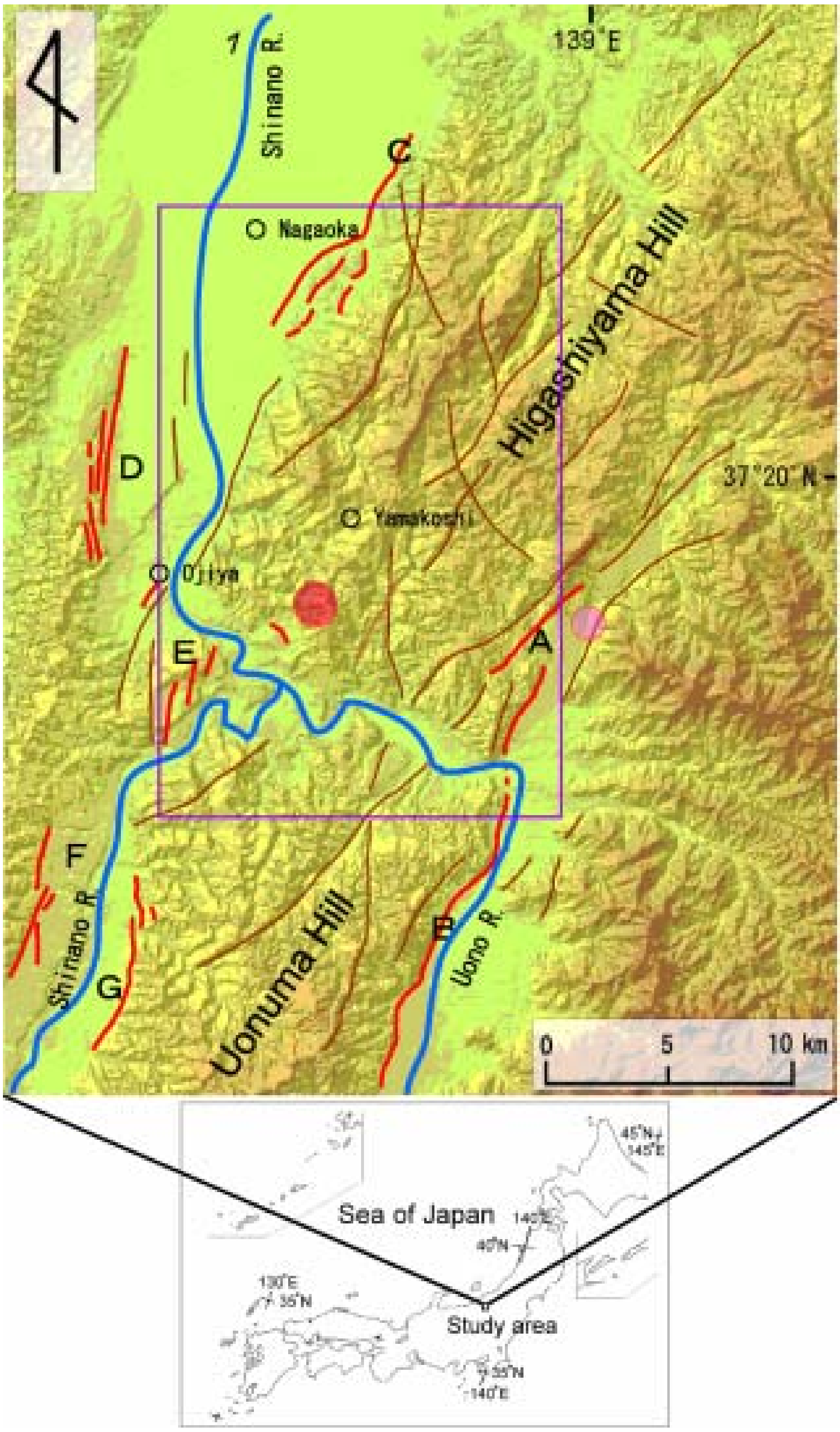

Fig.1 Study area. Bold line with **A**-**G**: known active faults ([4], [5], [6]), thin line on the Hills: lineament determined from aerial photos-interpretation, dark red dot: mainshock epicenter (October 23), pale-pink dot: aftershock epicenter (October 27), **A**: Obiro fault, **B**: Muikamachi fault, **C**: Yukyuzan fault, **D**: Katagai fault, **E**: Yamamotoyama fault, **F**: Tokamachi-west fault, **G**: Tokamachi-east fault.

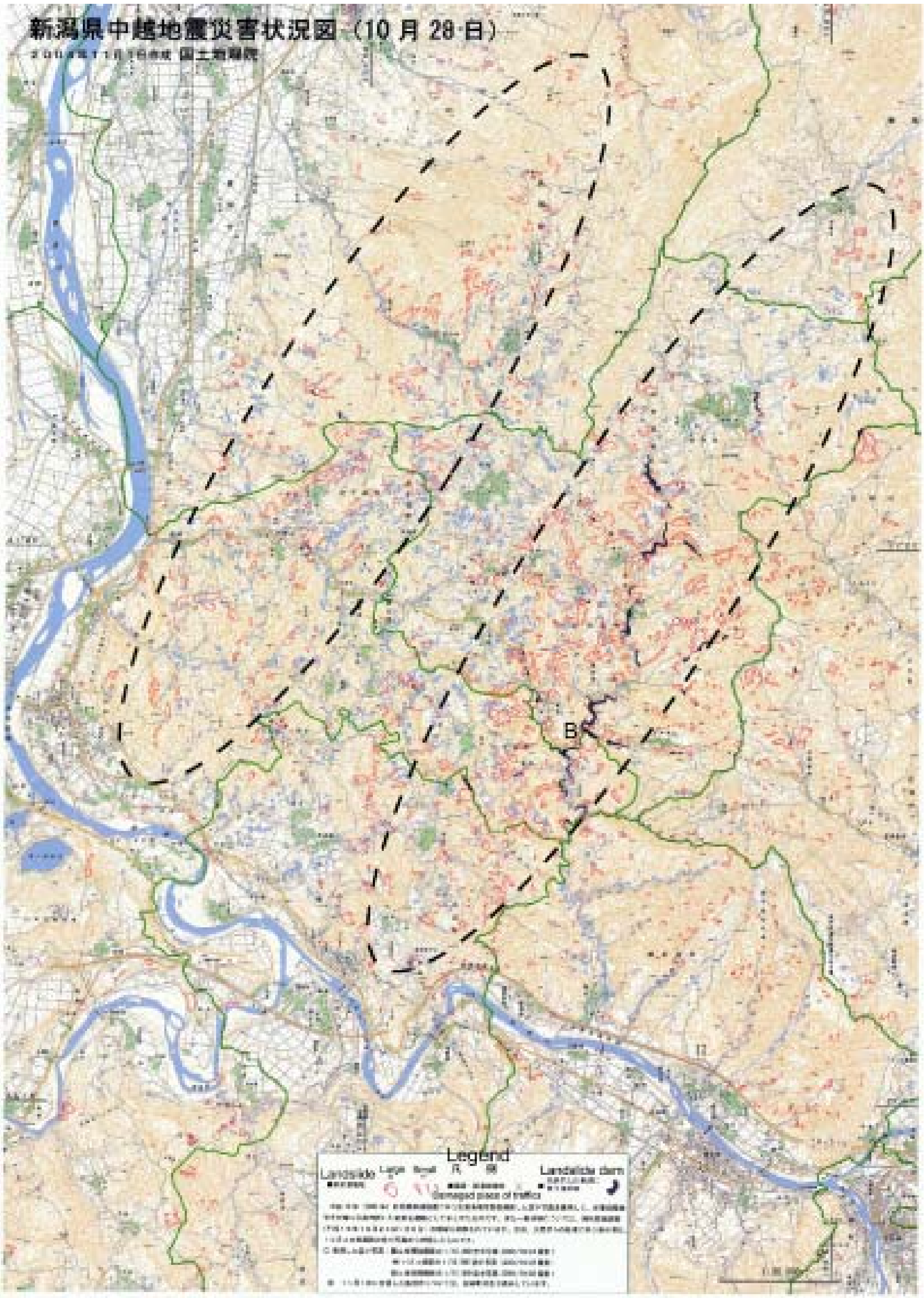

Fig. 2 Distribution of landslides triggered by the earthquake. Mapped landslide dams indicate the areas as of October 28, 2004. Black dotted lines and site “B” were added on the original “Disaster Map” (Geographical Survey Institute [10]).

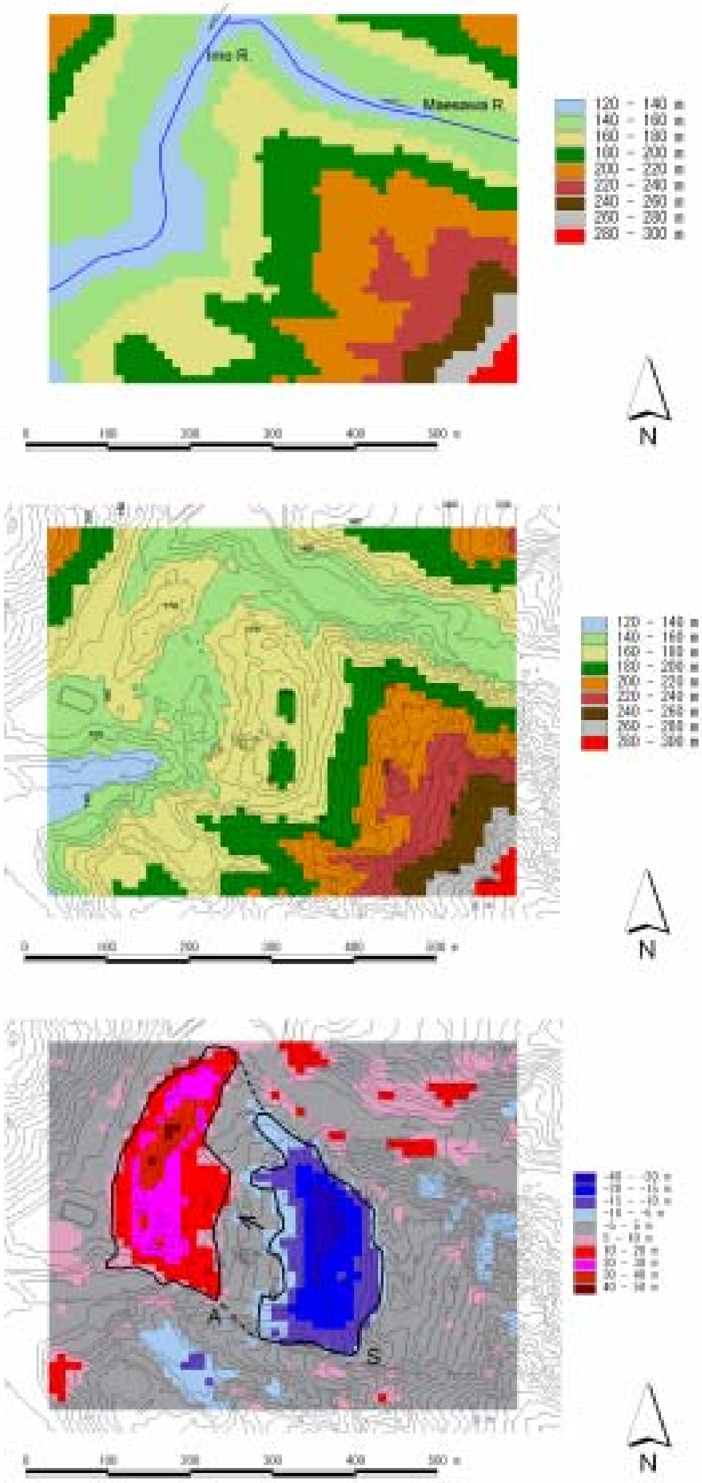

Fig. 3 Topography change between pre- and post-earthquake. The pre-earthquake DEM (upper) was derived from 1:25:000 contour map. In the middle figure, the post-earthquake DEM is superimposed on the contour lines, which were derived from the airborne LIDAR data, are in meters.

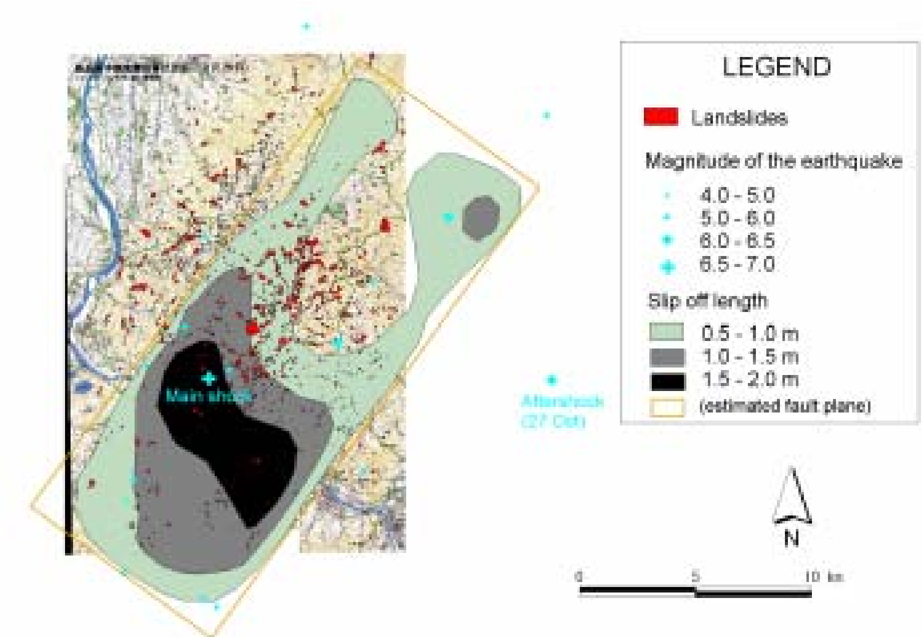

Fig. 4 Overlap of landslides distribution on the seismological data (magnitude data, [1]; calculated fault plane and slip off length, [3]).

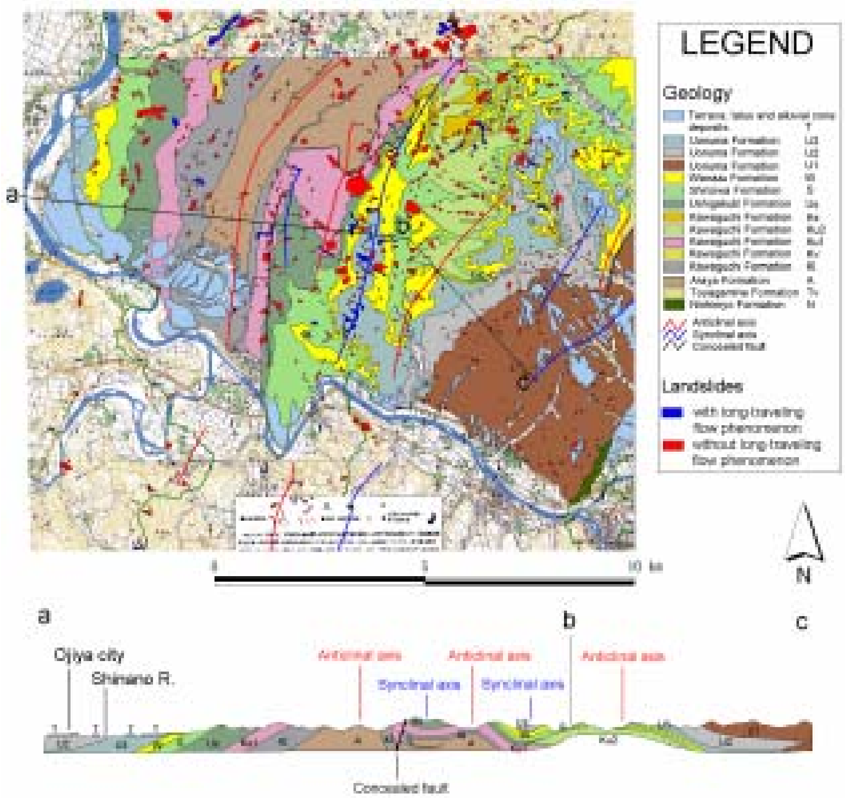

Fig. 5 Overlay of landslide distribution over the geological map. The geological map and cross section of the geology are a part of [7].

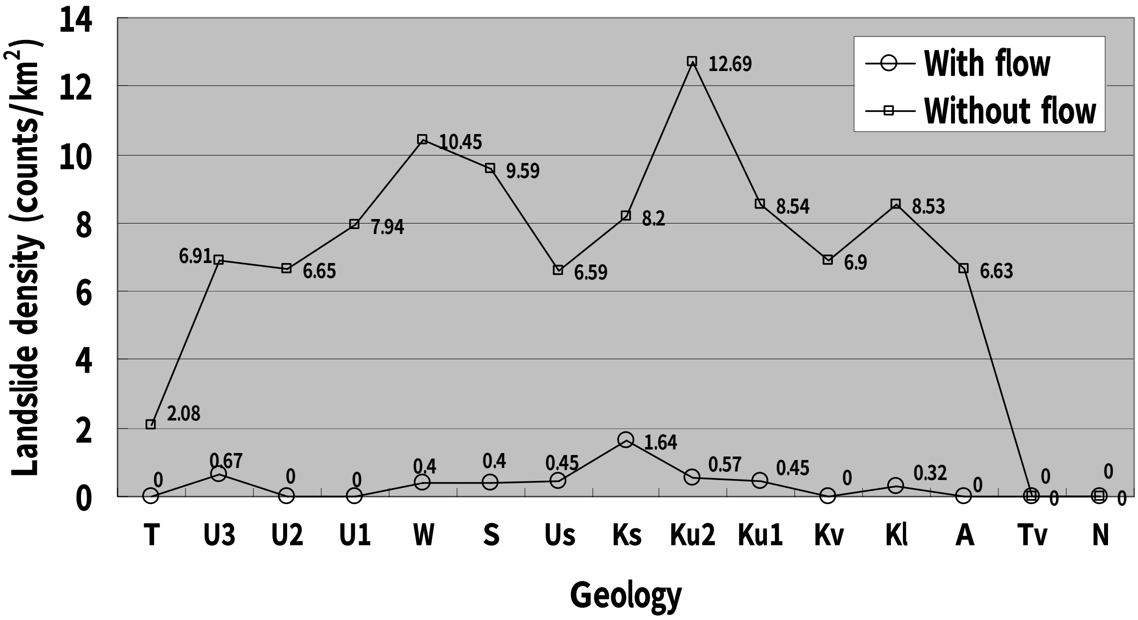

Fig. 6 Landslide density in each geological formation, correspondent to Table 1 and Fig. 5.